Scientia Iranica D (2023) 30(4), 1382–1398

Sharif University of Technology
Scientia Iranica
Transactions D: Computer Science & Engineering and Electrical Engineering
http://scientiairanica.sharif.edu

Research Note

A comparative study of lithium-ion battery and Pb-acid battery-supercapacitor hybrid energy storage system for frequency control and energy management of islanded microgrids

A. Karimi Rizvandi[a], M. Bagheri Sanjareh[b], M.H. Nazari[c,*], G.B. Gharehpetian[c], and S.H. Hosseinian[c]

a. *Department of Electrical Engineering, Iran University of Science and Technology, Tehran, 1311416846, Iran.*
b. *Department of Electrical Engineering, Shahid Beheshti University, Tehran, 1983969411, Iran.*
c. *Department of Electrical Engineering, Amirkabir University of Technology, Tehran, 1591634311, Iran.*

Received 18 March 2021; received in revised form 20 July 2021; accepted 8 November 2021

KEYWORDS
Microgrid;
Frequency control;
Energy management system;
Islanded operation;
Hybrid energy system;
Battery energy storage;
Supercapacitor;
Lithium battery;
Pb-acid battery.

Abstract. Among a variety of storage technologies used for energy storage systems, supercapacitors, Pb-Acid Batteries (PABs), and Lithium Batteries (LBs) are widely used for microgrid applications. The supercapacitors with high-power density are suitable for fast power regulations; conversely, the PABs have high-energy density, which makes them suitable for long-term energy management. Since the PABs and supercapacitor can complement each other and overcome mutual deficiencies, their combination as a hybrid energy storage system can be beneficial. However, the LB enjoys both high-energy and high-power densities. Therefore, an LB ESS (LBESS) can similarly function like a Pb-acid battery-Supercapacitor Hybrid ESS (PSHESS). However, their topologies, life cycles, and costs are different. This study tends to determine the one which is technically and economically more suitable for applications in islanded microgrids. For this purpose, a frequency control and energy management scheme is proposed. It maintains the balance between demand and supply and also keeps the microgrid frequency within safe operational limits using the least needed sizes for the energy storage systems. Using the simulation results, the sizes and costs of the energy storage systems are determined. For a decade of operation, the PSHESS has incurred almost 49.2% more cost than the LBESS, which makes the LBESS more cost effective.

1. Introduction

Micro-Grid (MG) is a group of interconnected distributed energy sources and loads. An MG can be connected to or disconnected from the upstream network to operate in a grid-connected or islanded mode. As long as the MG is connected to the upstream network, the upstream network keeps the supply-demand balance in the MG and maintains the MG frequency within a tight range. However, in the islanded mode, the power generation and consumption of MG may not be balanced [1,2]. A low-inertia MG can experience large frequency deviations [1,3]. Installation of an energy storage system with a fast-responding capability to inject/absorb is a solution to keep the

*. *Corresponding author.*
E-mail address: nazary@aut.ac.ir (M.H. Nazari)

doi: 10.24200/sci.2021.57928.5476

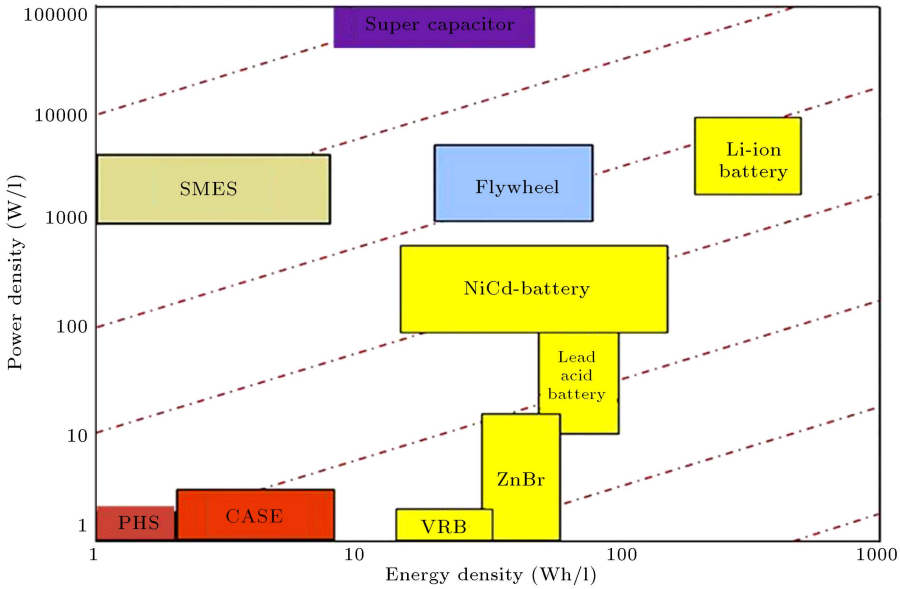

Figure 1. Classification of most common ESSs [9].

supply-demand balance in the islanded MG [4,5]. The energy and power densities are important features of ESS technology [6,7]. The energy and power densities of the most common ESS technologies are presented in Figure 1. The ESSs with high power density are capable of fast discharging/charging energy, which makes them suitable for fast power regulations. On the contrary, the ESSs with high energy density are capable of discharging/charging power for a long period but not with high discharge/charge rates [8]. Batteries are one of the most widely used ESS technologies because they are cost-effective and easy to use [9,10]. Among them, Pb-Acid Battery (PAB) is the most widely used battery technology for grid applications [11,12].

The Southern California Edison Company installed a 40-MWh PAB at a substation in Chino that was used for a variety of different applications including VAR control, frequency control, voltage control, black-start transmission line support, spinning reserve, load following, load levelling, and peak shaving. A PAB was also utilized in Metlakatla, a small community on an island off the coast of Alaska whose power needs are supplied by a diesel-powered generator and a hydroelectric generator. However, since the use of diesel generator was not economically feasible, it was replaced by a PAB. Further analysis of the system indicated that the PAB could improve the power quality and stability by reducing both frequency and voltage variations. Moreover, in the Shetland Isles in Scotland, a PAB with 3-MWh capacity was installed alongside a diesel generating plant and a wind power plant. The aim of using the PAB is to reduce demand for diesel generation and increase the proportion of wind power, which can be used. Since the year 2013 when the system was first installed, it has been operating successfully, thus improving the power quality and reducing the peak demand by 20%. Another case of PAB usage in grid applications is Hydro Tasmania, an electricity utility in Australia. It integrates a PAB with renewable Distributed Generators (DGs) to ensure the uninterruptible supply of island demands such as residential and commercial loads [13].

In [14], a PAB-SC Hybrid ESS (PSHESS) was used for energy management and compensation for the demand-supply mismatch in the islanded MG with renewable DGs. The rationale behind hybridizing the PAB with the Supercapacitor (SC) is that the PAB is not a high-powered ESS. It means that if it is utilized for short-term power regulations like frequency control, it will face the aging problem which significantly increases the replacement cost. Therefore, it is recommended that a high-powered ESS, mostly a SC, be used in parallel with the PAB as a Hybrid ESS (HESS), which increases the PAB lifetime by using the SC and PAB for fast and slow power regulations, respectively [9,14]. To this end, in [14], a low-pass filter was employed to separate the Slow and Fast Components of the MG Frequency Variations (SCMFVs and FCMFVs) so that the PAB and SC could handle slow and fast power regulations, respectively. In this study, the low- and high-pass filters are used based on the same approach, as presented in [14].

A HESS can be configured in active, passive, or combined form of either in series or in parallel. Figure 2 shows the most common HESS topologies [15]. For passive connection, the terminals of the ESSs are directly connected to the DC bus. In this case, the power sharing mechanism and response are determined by the electrical characteristic of the HESS elements. In semi-active topologies, one of the HESS elements is

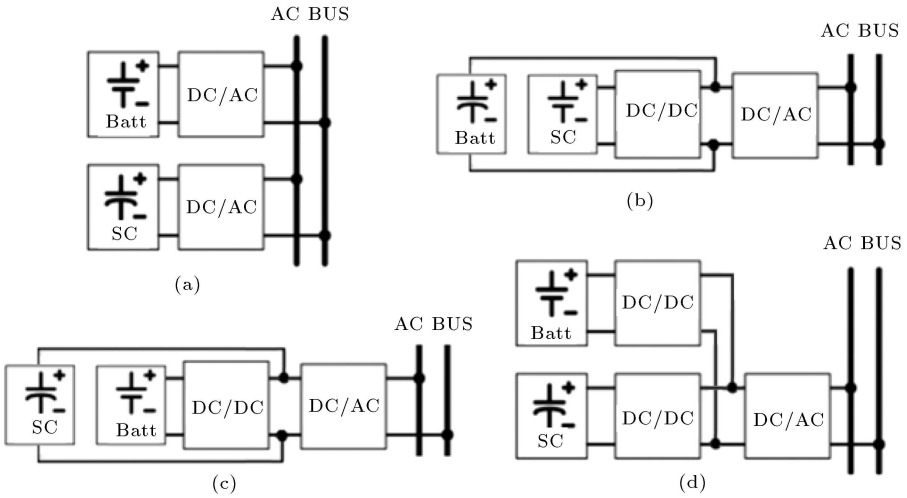

Figure 2. Classification of Batter-SC HESS topologies. (a) Passive, (b) Supercapacitor semi-active HESS, (c) Battery semi-active HESS, and (d) Active topology.

directly connected to the DC bus, while the other one is connected via a bi-directional DC/DC power converter. In active HESS topology, the bi-directional DC/DC power converters are employed to actively control the power flow of each HESS element [14]. Sophisticated control schemes can be implemented in a fully active HESS which is the most commonly used configuration [16]. Of note, they have some deficiencies including high complexity, increased losses, and high cost, most importantly.

Another alternative to both long-term energy management and short-term power regulation is the use of ESS with both high power and energy densities like Lithium-Ion Battery (LIB) [17]. A 63-MWh LIB alongside wind and solar power plants was installed in northern China to perform demand shifting and frequency regulation. Meanwhile, in order to improve the balance between the demand and renewable power generation, Tohoku Minami-Soma Substation installed a 40-MWh LIB storage in Japan [18]. In [19], the LIB was utilized for load levelling and peak shaving. In [20], the high power characteristics of the LIB were taken into consideration for the frequency control of an islanded MG. Findings in [18–20] demonstrated the suitability of the LIB for both short-term fast power regulations and long-term energy management. Figure 3 shows the topology of an LIB ESS (LIBESS), which mainly consists of an LIB, a DC/DC bidirectional converter, and an inverter. In comparison to the active topology of the PSHESS, the LIBESS requires one less converter, which makes it less expensive. In addition, LIBs have longer lifetime. However, their initial cost is much higher than that of PABs.

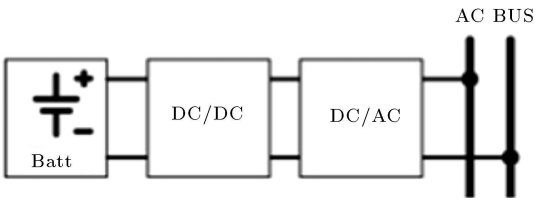

Figure 3. LIBESS topology.

In [21], the effect of fast charge/discharge or charge/discharge with high rates on the LIB life cycle was investigated. As mentioned in [22], the reduction of its cycle life is closely related to the heating of the cells due to high current rates. In [23], an aging evaluation was experimentally performed on high-powered LIBs, which were subjected to micro-cycles. The micro-cycles are discharge/charge cycles at high currents distinguished by a variation of State of Charge (SOC) lower than 5%. Evaluation of the experimental aging reveals that high discharging/charging currents up to ten times the nominal currents, which lasted for almost tens of seconds in durations, do not cause a considerable thermal stress on the LIB cell. In addition, the LIB cell can perform hundreds of thousands of micro-cycles before causing a considerable degradation. The life cycle of an SC is also in the order of hundreds of thousands [23], proving that the participation of LIBs in fast power regulations, lasting for tens of seconds, has no effect on their aging. In other words, an LIBESS can simply function like a PSHESS without any problems. In fact, degradation results obtained in [22] were valid for full discharge cycles at constant high rates compared to shallow cycles within short periods.

In [1], a Frequency Control and Energy Management (FCEM) scheme was proposed for islanded operation of a greenhouse MG. Of note, the adequate size of the BESS for these tasks was not determined in this study; instead, in case of insufficient power generation and low SOC of the battery, load reduction was imposed to match the supply and demand. In [24], a coordinated control scheme was proposed using an HESS for energy management of a microgrid in

the islanded mode. In addition, the sufficient size of the HESS for islanded operation of MG was not determined, and the dispatchable DGs were not used alongside the HESS. These drawbacks could lead to under-discharging and over-discharging of the battery so that in order to solve this problem, the authors proposed load shedding and curtailment of the power of renewable DGs. In addition, they did not propose an HESS sizing methodology. Unlike [1,24], in this study, the proposed FCEM for islanded operation of MG was used to size PSHESS, while all loads were continuously supplied. In addition, unlike [24], renewable DGs generated their maximum available power without reaching the battery SOC limits. Therefore, the undesired actions like load shedding and curtailment of renewable DGs power were prevented. Random sizing of ESSs can cause some specific problems such as incurring unnecessary high costs due to the oversizing of the ESS power rating and capacity. Therefore, an ESS sizing approach is needed to size the ESS with the minimal size to achieve the desired goals. In [25,26], in order to minimize the BESS cost, short-term frequency regulation studies were performed to determine the minimal needed capacity and nominal power of the BESS for MG operation in an islanded mode. However, the methodology used for determining the nominal power and capacity of the BESS was not clearly described. In [27], a novel approach was proposed to determine the minimal power rating of the LIBESS required to keep the MG frequency deviations within the allowable range. Since keeping the supply-demand balance is essential in the islanded MG [28], energy management simulations should be performed to determine the needed capacity of the BESS for this task, which were not conducted in [25–27]. In order to determine the power rating of the ESS, both energy management and frequency regulation studies are necessary. The power rating of the ESS is equal to the maximum of needed power ratings resulting from both studies. In order to calculate the ratings of the ESS elements, both long-term energy management and short-term frequency regulation studies were carried out.

In [29], the optimal size of the HESS elements was determined to keep the supply-demand balance in an islanded MG with renewable energies. Gbadegesin et al. determined the size and cost of PSHESS to minimize the MG operational cost in the islanded mode [30]. The control strategy for using a battery-SC HESS is to reduce fast power regulation on the battery by using the SC and the battery used for fast and slow power regulations, respectively. However, in [29,30], the SC and the battery for both fast and slow power regulations were concurrently used, which were against the rationale behind the hybridization of the battery with SC. Moreover, frequency regulation studies were not carried out in [29,30] to calculate the needed power rating of the HESSs for the MG islanded operation. The most important feature of this work is to consider the capability of LIBs to perform microcycles for fast power regulation, which was not covered in the previous studies like [24,29,30]. Through this capability, the LIBs can perform both fast and slow power regulations that fundamentally question the necessity of using the PSHESSs since the LIBESS can simply function like one.

Considering that both LIBESS and PSHESS can handle short-term fast power regulations and long-term energy management, this research paper aimed to conduct a techno-economical comparative study between them to determine which one is more suitable. In this regard, two FCEM schemes were designed for islanded MG operation based on different topologies and control systems of the LIBESS and PSHESS. Using these schemes, the simulation studies of the FCEM of the islanded MG were performed using LIBESS and PSHESS. Then, based on the simulation results, their size and cost were evaluated and compared for the MG operation during the islanded mode. The main contributions of this paper are listed in the following:

- Previous studies such as [29,30] have mainly focused on the economic or technical issues of the HESSs for both fast and slow power regulations. This paper, however, proposes that in addition to the HESSs, the LIBESSs are also suitable for performing these tasks. In this regard, the PSHESS, which is one of the most commonly used HESS technologies, is technically and economically compared with the LIBESS with the objective of discovering whether or not the LIBESS is the superior candidate for FCEM of the islanded MGs;
- In order to determine the ESS dimensions for the MG islanded operation, it is necessary to perform both frequency regulation and energy management studies to ensure that ESSs can handle both of them. However, the studies in [25,26,29] determined the ESS dimension using one of these studies. In this paper, both energy management and frequency regulation studies were conducted to size the dimensions of both PSHESS and LIBESS. For this purpose, two FCEM schemes are proposed, which determine the minimal sizes of the PSHESS and LIBESS for keeping the supply-demand balance and keeping the MG frequency deviations within an allowable range during islanding;
- A sizing and cost evaluation procedure is presented in this study, which helps making a techno-economic comparison between the PSHESS and LIBESS for a decade of operation.

The overall outline of the manuscript is presented in Figure 4. In Section 2, the proposed FCEM

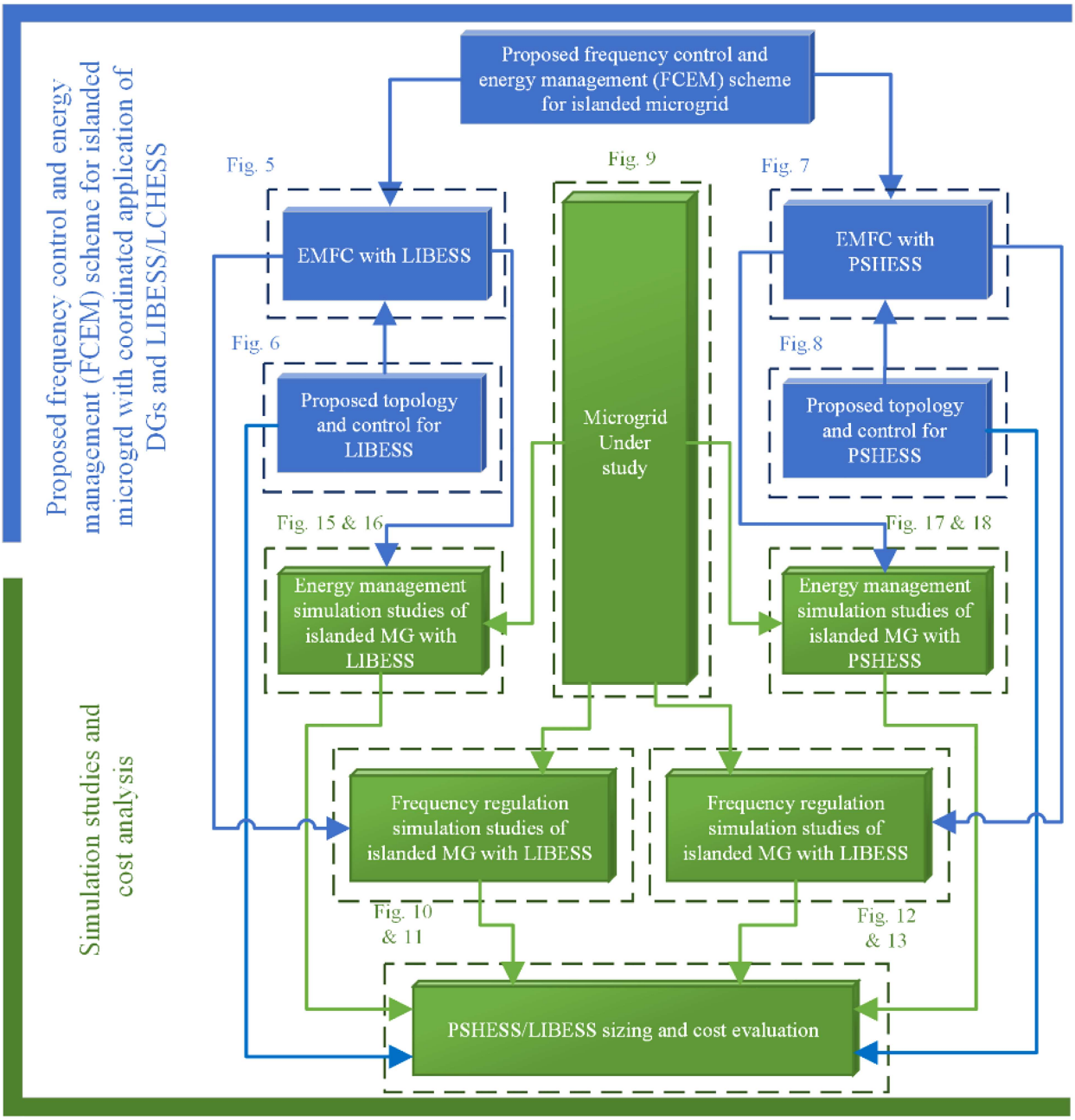

Figure 4. LIBESS topology.

schemes are described based on the topologies and control systems of LIBESS and PSHESS. In Section 3, the proposed FCEM scheme is evaluated using the simulation studies. In Section 4, the sizing and cost analysis of LIBESS and PSHESS are presented.

2. Proposed FCEM

As far as the MG is connected to the upstream network, the load-generation balance is guaranteed and thus, the frequency is kept in an acceptable range. In the islanded mode, however, the MG may undergo rapid frequency deviations due to the load variations, sporadic nature of renewable sources, absence of upstream network, etc. The dynamics of the MG frequency can be modeled using Eq. (1) [31,32]:

$$\frac{df}{dt} = \frac{f_0}{2\sum H_i}(P_G - P_D), \tag{2.1}$$

where P_D is the total demand of MG, P_G the total power generation of the MG, and $\sum H_i$ the sum of all rotating machines in the MG. In addition, f and

f_0 are the frequencies of the islanded MG and its rated value, respectively. The MG energy sources are responsible for keeping the supply-demand balance during the islanded operation. The DGs with large time constant and slow response are not able to handle the frequency control. Moreover, considering that the DGs may not be able to provide the total needed power generation during the peak period, it is imperative to utilize an ESS to compensate for the supply-demand mismatch. During the islanded operation, the ESS control strategy for energy management is discharging during periods with high power demand and charging during periods with low power demands as well. The heavy load profile of the mid-summer is considered as the worst case of energy management for sizing the ESS capacity. If the BESS can compensate for the supply-demand mismatch in this case, it can undoubtedly handle the energy management of the islanded MG in other less severe cases, as well. Moreover, the ESS should be able to inject/absorb the maximum needed power in the cases with the most severe power shortage/surplus to keep the frequency deviations within an allowable range. In fact, both energy management and frequency regulations must be performed to determine the capacity and power rating of the ESS.

2.1. FCM using LIBESS

Figure 5 shows the control system and configuration of a grid-connected LIBESS. The main components of the LIBESS are the LIB, filters, inverter, and DC/DC converter. The control of charge/discharge control of the LIB using the DC/DC converter was elaborated in [33] in detail. The LIBESS power setpoint is denoted by P_{batref}. As long as the MG is connected to the upstream network, P_{batref} is determined by the control center of MG. I should be noted that during the islanded operation, the frequency controller of the LIBESS, which is Proportional-Integral (PI), defines P_{batref}. In case the DGs generate their maximum power generation capacity, the proportional controller is just functional and the integral controller is disabled.

The conventional dq current controller is used for controlling the inverter, as fully discussed in [24,34,35]. The output active and reactive powers of the inverter are denoted by I_{qref} and I_{dref}, respectively. The voltage of DC link (V_{DC}) between the inverter and the converter is kept at the reference value (V_{DCref}). For this purpose, I_{dref} is regulated using a PI controller. In order to absorb power from the MG, the converter is controlled to absorb energy from the DC link, which leads to a decrease in V_{DC}. The inverter absorbs energy from the MG to increase and maintain V_{DC} at V_{DCref}. Contrarily, in order to inject power to the MG, the converter is controlled to inject energy to the DC link from the battery, which leads to an increase in V_{DC}. The inverter injects energy to the MG to maintain V_{DC} at V_{DCref}. As the FCEM studies mainly deal with the active power, the LIBESS is controlled to operate at unity power factor by setting I_{qref} to zero [35].

Figure 6 shows the coordination of the DGs and LIBESS for FCEM of the islanded MG, which can be obtained from Equation (1). The outputs of the DGs and energy sources denote their power generation, while the inputs of dispatchable DGs denote their power setpoints. The blocks of renewable DGs do not have inputs to receive power setpoints because they always produce their maximum power. The frequency of the islanded MG is stable as long as the balance between supply and demand is maintained. The frequency control consists of two stages of primary and secondary frequency. In the primary stage, the fast-responding LIBESS intercepts frequency using a proportional controller with the gain of $K_{LIBESS1}$. In the secondary stage, the dispatchable and slow-responding DGs gradually change their power generation to compensate the supply-demand mismatch to restore the frequency at its nominal value. Here, K_{dis} denotes the gain of integral controller used to share the supply-demand mismatch between the dispatchable

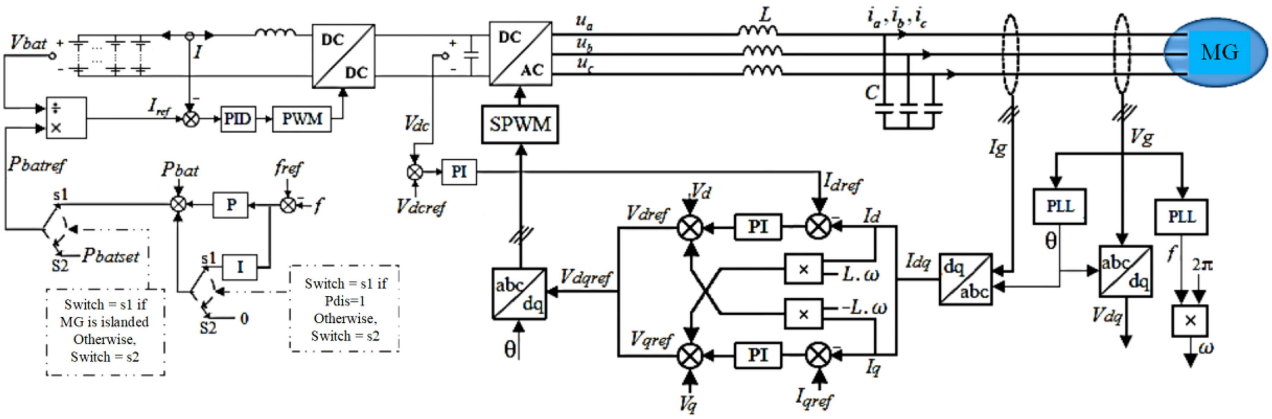

Figure 5. Configuration and control system of a grid-connected LIBESS.

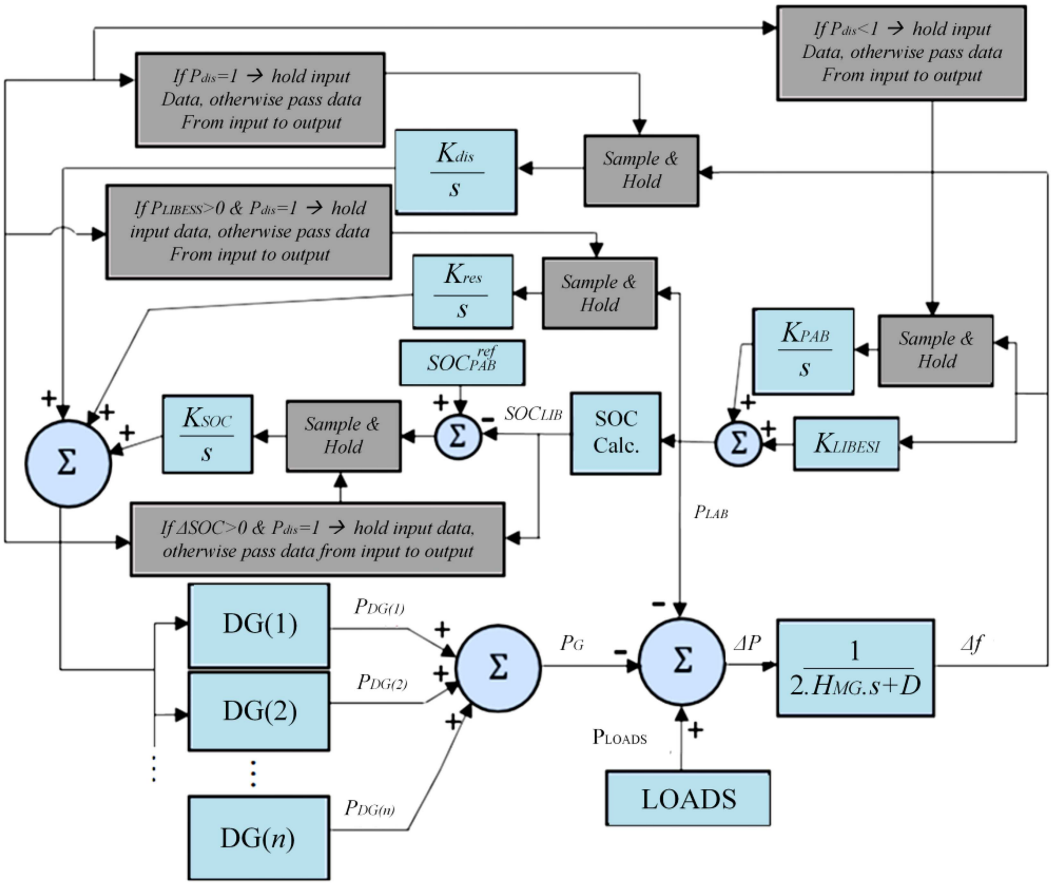

Figure 6. FCEM schematic of the islanded MG with cooperative application of the LIBESS and DGs.

DGs. If the dispatchable DGs reach their maximum power generation limits, the residual supply-demand mismatch is provided by the LIBESS using an integral controller with the gain of K_{LIBESS}. In case the power generation of dispatchable DGs is below the maximum limits, an integral controller with the gain of K_{res} is used to bring the power of the LIBESS back to zero. Upon decreasing/increasing $K_{LIBESS1}$, the absorption/injection rate of LIBESS power in response to the frequency deviation decreases/increases, respectively. Moreover, increasing the absorption/injection rate of the LIBESS power decreases the frequency deviation. The allowable range for the variations in the MG frequency is ±1% of the nominal value [36]. In this regard, $K_{LIBESS1}$ is adjusted to provide enough LIBESS power injection/absorption to keep the frequency of the islanded MG within the allowable range. For this purpose, the worst power shortage/surplus case studies were taken into account to permanently determine the value of $K_{LIBESS1}$. In doing this, the frequency of the islanded MG will also be maintained within the permissible limits in less severe contingencies. The minimum and maximum limits for (LIB SOC $(SOC)_{LIB}$) were calculated as 20% and 80%, respectively [37]. If SOC_{LIB} reaches 80%, it will not absorb more power and if it reaches 20%, the LIBESS will not inject more power, except that SOC_{LIB} returns within these limits. The integral controller with the gain of K_{SOC} is used to control the power of the DGs to adjust SOC_{LIB} at its reference value (SOC^{ref}_{LIB}). It is worth noting that the controller SOC_{LIB} tries to absorb (inject) the total injected (absorbed) LIB energy, while the power dispatch controller (K_{LIBESS}) merely tries to quickly share the LIBESS power between the DGs.

2.2. FCM using PSHESS

Figure 7 shows the control system and configuration of a grid-connected PSHESS connected to the MG. The main components of the PSHESS are the LIB, SC, filters, inverter, and DC/DC converter. The control systems of the inverter, converters, and charge/discharge controllers of both SC and PAB are almost the same as those of LIBESS discussed in Section 2.1. Moreover, the frequency controller of both SC and PAB is also the same as that of the LIBESS, except that the high-pass and low-pass filters are used in their frequency controllers such that they only respond to FCMFVs and SCMFVs, respectively. The filters time constants (T) are set to 1.5 sec, as suggested in [14]. A PI controller is also used in each of the power controllers of the SC and PAB to keep the SOC of SC (SOC_{SC}) at its reference value (SOC^{ref}_{SC}). In case the SOC_{SC} is

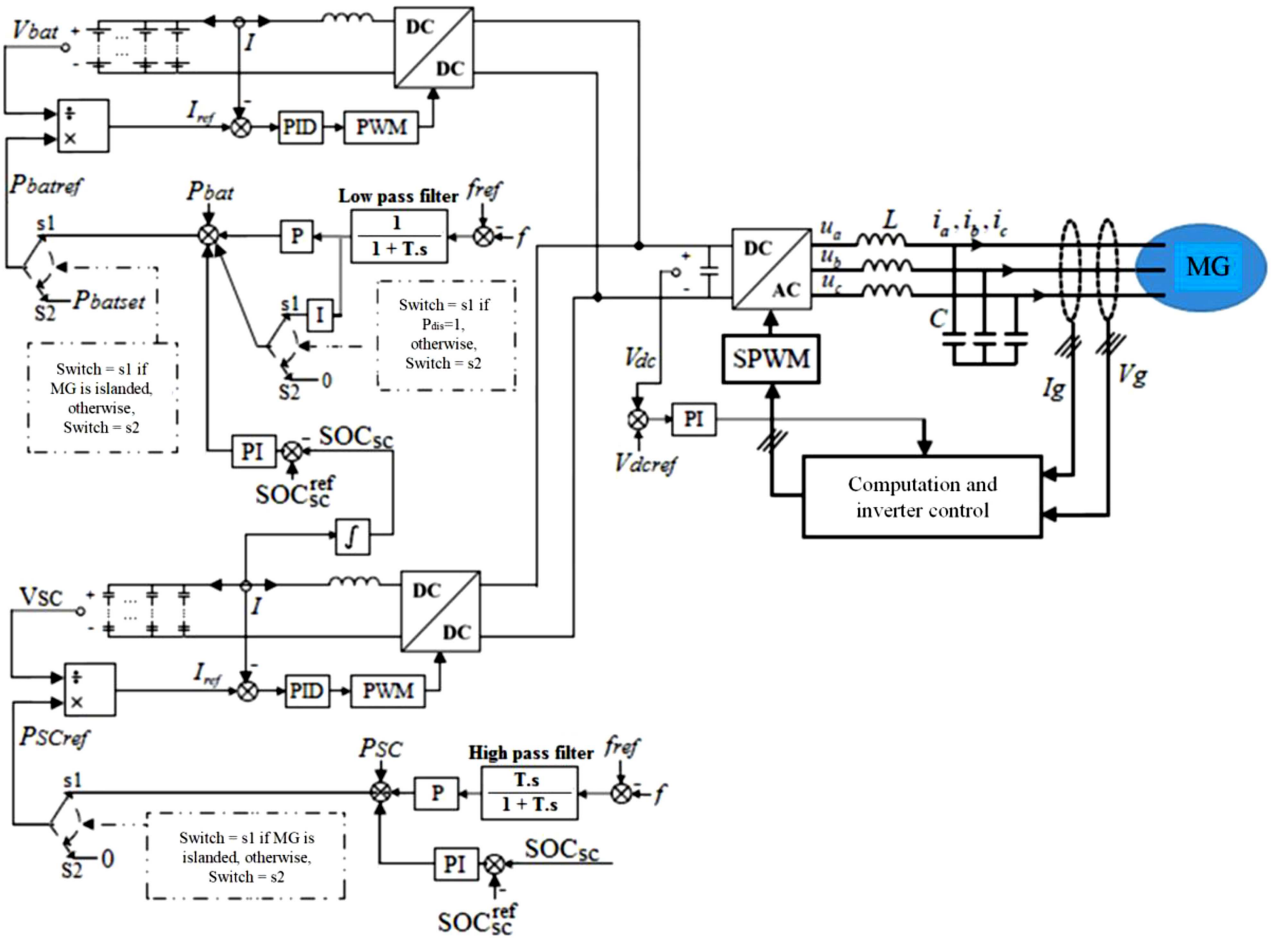

Figure 7. Configuration and control system of a grid-connected PSHESS.

above SOC_{SC}^{ref}, the PAB absorbs the discharged energy of the SC through the DC link. On the contrary, in case the SOC_{SC} is below SOC_{SC}^{ref}, the SC absorbs the PAB discharged energy. In comparison to the LIBESS, the control system and configuration of the PSHESS are much more complicated, which is the drawback of the PSHESS.

Figure 8 shows the coordination of the DGs and LIBESS for the FCEM of the islanded MG, which is obtained based on Eq. (1). The PSHESS control is almost similar to the LIBESS control, except that the SC does not participate in energy management and frequency restoration and merely responds to FCMFVs using a high-pass filter, while the PAB just responds to SCMFVs using the low-pass filter. The tuning of the proportional controller of the PSHESS (K_{SC}), like $K_{LIBESS1}$ in Section 2.1, is used for keeping the frequency deviations within the allowable range.

3. Simulation studies

In order to size the LIBESS and PSHESS, both energy management and frequency regulation studies should be conducted. For this purpose, the first part of this section introduces the MG network, which is used for simulation studies. In the second and third parts, the simulation studies of the frequency regulation and energy management are performed, respectively. The sizes of the elements of SBHESS and LIBESS were initially chosen large enough to successfully perform their tasks during the simulation studies. Then, in accordance with the simulation results, their sizes will be determined to specify the overriding candidate for the islanded MG applications.

3.1. MG specification

The MG network under study is the CIGRE low-voltage MG [20,38], which is presented in Figure 9. It includes a Diesel Engine Generator (DEG), a Microturbine (MT), and a Solid-Oxide Fuel Cell (SOFC) at power ratings of 31.1 kW, 31.1 kW, and 10 kW, respectively. There are also two Photovoltaic (PV) systems and an ESS in the MG. The PV systems generate 2.7 kW and 9.3 kW at a solar radiation intensity of 1000 W/m^2 and a temperature of 35°C. The power generation capacity of the DGs, excluding the PVs, is 72.2 kW.

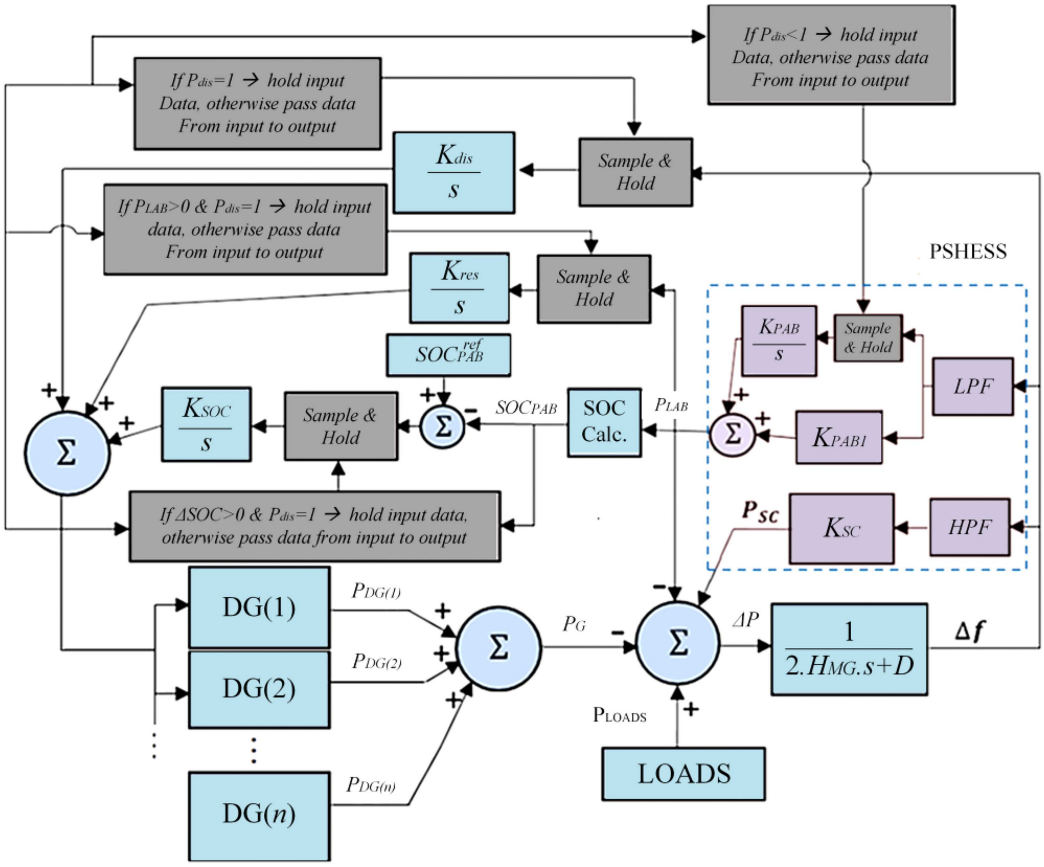

Figure 8. FCEM schematic for islanded operation of MG using cooperative application of PSHESS and DGs.

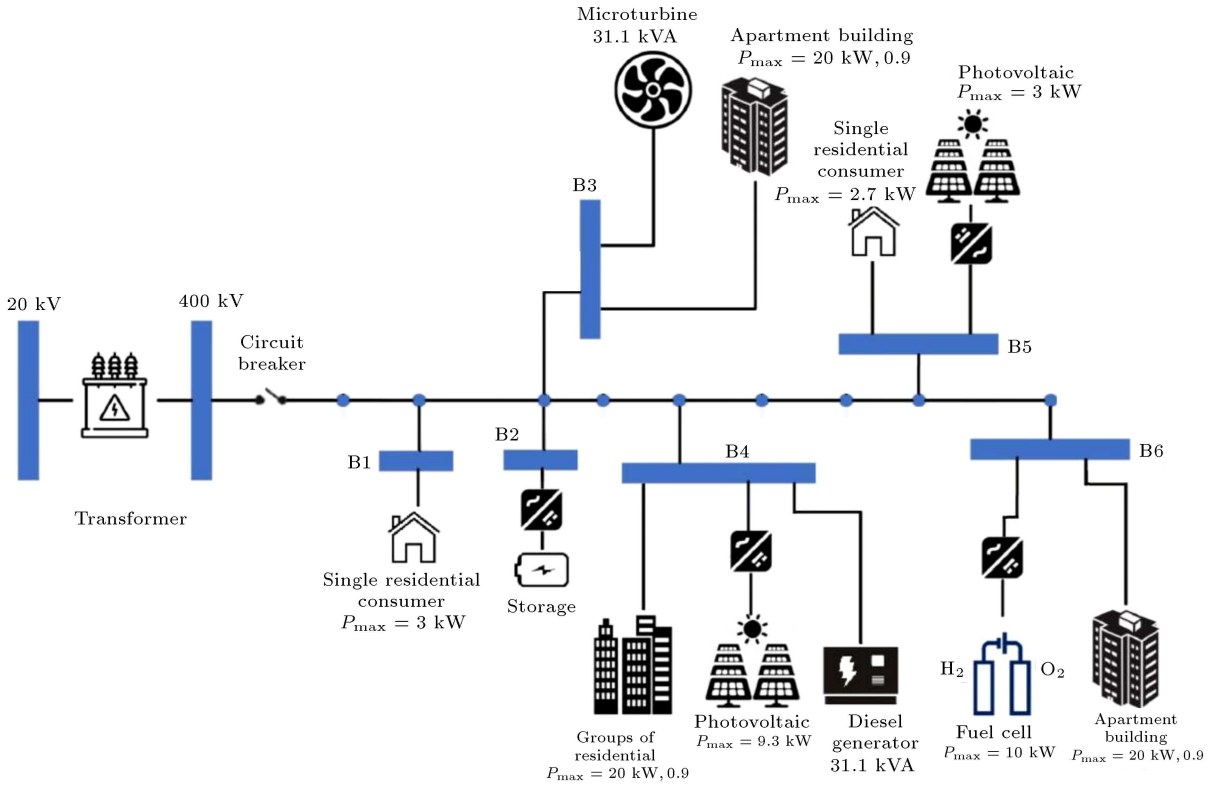

Figure 9. MG under study.

3.2. Frequency control simulation studies

According to [27,35], the shortage of 20 kW power generation after the unexpected islanding can be regarded as the worst frequency disturbance that can occur in the MG under study. The DEG model used for frequency control studies is available in [39] while the MT and the SOFC models are taken from [40]. The presented model and controllers in Section 2 are used to model the LIBESS and PSHESS while the available model in MATLAB/Simulink software is used for the PV systems.

3.2.1. Frequency regulation using LIBESS

A disturbance occurs in the utility grid such that in order to keep the stability of the MG, it should continue its operation in the islanded mode at the 5th second, while it is still importing 20 kW power from the utility grid. The total power consumption of the MG and total power generation of the DGs before islanding were calculated as 64.9 kW and 44.9 kW, respectively. Figure 10 shows that the frequency of the islanded MG drops after the occurrence of power shortage. As observed in Figure 11, the LIBESS quickly discharges the maximum power of 28.69 kW, which results in the frequency interception of 49.501 Hz. Of note, in order to keep the MG frequency above the lower frequency limit (49.500 Hz), K_{LIBESS} should be adjusted to 57.334. The MT, DEG, and SOFC gradually increase their power generation to permanently compensate 20 kW power shortage, which eventually results in the frequency restoration of 50 Hz. The power of the LIBESS is also restored at 0 kW.

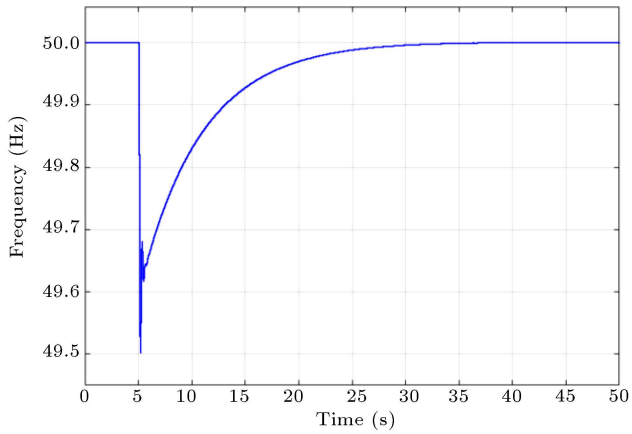

Figure 10. MG frequency.

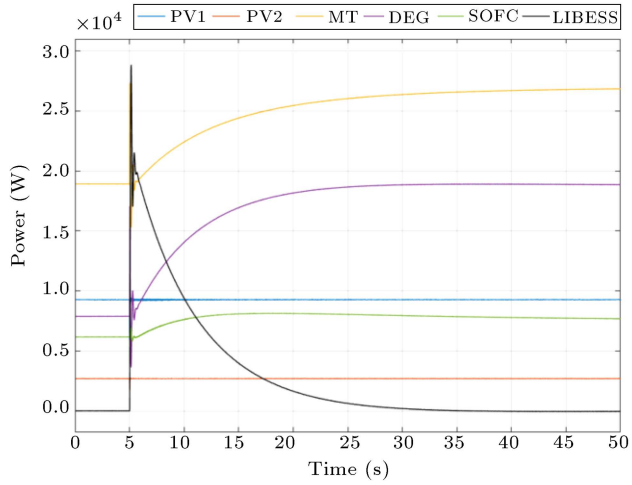

Figure 11. Power generation of DGs and LIBESS.

3.2.2. Frequency regulation using PSHESS

The scenario and the disturbance are similar to those in Section 3.2.1. Figure 12 shows the power generation of DGs. Figure 13 shows the MG frequency, which drops due to the power shortage. In order to keep the frequency of the MG deviation above 49.50 Hz, the SC quickly discharges the maximum power of 27.61 kW. It should be noted that K_{SC} was adjusted to 57.334. Unlike the SC power, the PAB power was observed to undergo a gradual increase, reducing the stress of the fast power regulations on the PAB. This is the result of separating the FCMFVs from SCMFVs using high-pass

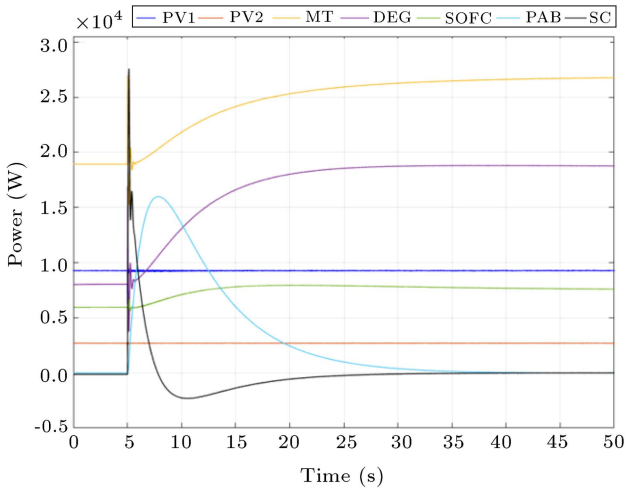

Figure 12. DGs power generation.

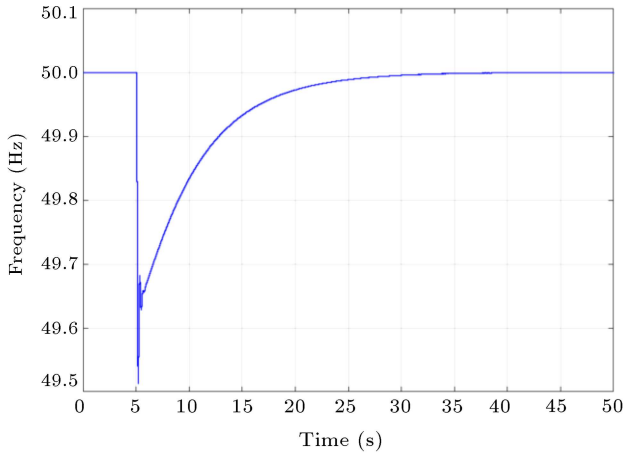

Figure 13. MG frequency.

and low-pass filters in the frequency controllers of the SC and PAB, respectively. The negligible difference between the maximum power of the LIBESS in the previous section and the maximum power of the SC is that the PAB slightly participated alongside the SC in fast power injection. Consequently, the peak power of the PSHESS was obtained as 28.69 kW similar to that of the LIBESS. The frequency eventually returned to its nominal value at the 50th second as the result of the permanent compensation of the 20 kW power shortage by the MT, DEG, and SOFC. The powers of the SC, PAB, and PSHESS also returned to 0 kW. From the 5th second until the frequency restoration, the SC discharges the energy amount of 5.6648 Wh and then, it absorbs the energy amount of 5.6361 Wh.

Given the discharge/charge efficiency of the converter, the discharged and charged energies of the SC are almost the same, making the SCO_{SC} remain near SOC_{SC}^{ref}. Also, the PAB power reference controller tries to maintain SCO_{SC} at SOC_{SC}^{ref}. From the 5th second till the moment that the PAB returned to 0 kW, it discharged the total energy amount of 45.0142 Wh. Of note, the maximum discharged power of PAB is 16.26 kW.

3.3. Energy management simulation studies

This section discusses the simulation studies for energy management of the islanded MG. During certain periods like the peak-load periods, the power generation capacity of the DGs might not be sufficient enough to provide the total power consumption of the islanded MG. The solution is to install an ESS that can be charged during the off-peak periods and discharged during peak-load periods. By doing this, the ESS and DGs can cooperatively provide the total power consumption during the peak-load periods. Here, using this strategy, the battery size is determined to ensure the supply of the MG loads without any interruption in a one-day period. The battery size is determined based on the heavy load profile of the mid-summer day, which is considered as the worst case that requires the most battery capacity for energy management. If the battery supplies the loads in this case, it can definitely handle energy management on other days with lighter load profiles. As the load profile data of the MG has not been presented in the previous works [20,27], the load profile in Figure 14 is used as the heaviest load profile that the MG annually experiences. Figure 14 also shows the values of power generation of the PVs during this period.

The MG model used in Section 3.2 is complicated which makes the runtime of the energy management simulation studies very long. Therefore, the simple models in Figures 5 and 6 are used instead to model the energy management of the islanded MG in Simulink. Compared to the model used in Section 3.2, this

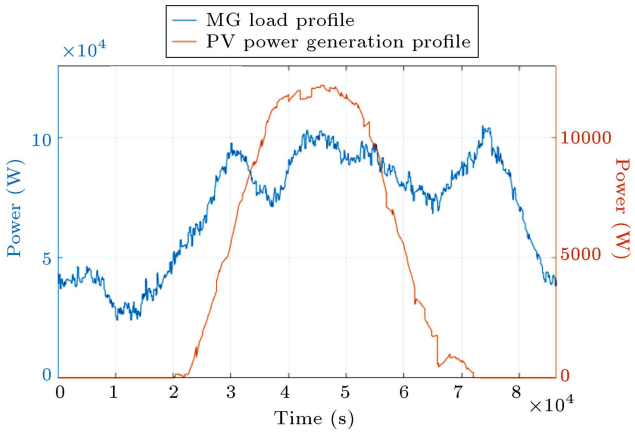

Figure 14. Data profile of MG demand and the power generation of PVs during mid-summer.

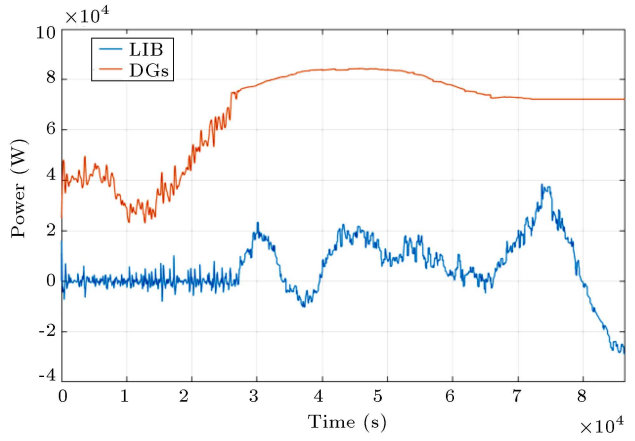

Figure 15. LIBESS and DGs power.

model is much simpler and faster to be simulated. For instance, in the simulations of the inverters, the dynamics of synchronous generators that are time consuming are not considered in this model. Therefore, this model is suitable for energy management studies. The DEG model is taken from [41,42], while the SOFC and MT models are available in [43].

3.3.1. Energy management with LIBESS

Figure 15 shows the LIBESS power and power generation of DGs. The discharged energy of the LIB minus its charged energy is shown Figure 16. From the beginning of the day until $t = 27200$ sec, the MG loads are supplied by the DGs, and the LIBESS mainly handles the primary frequency control. Figure 16 confirms that LIBESS does not participate in energy management because the total charged/discharged energy of the LIB until this moment is zero. However, from this moment until $t = 79761$ sec, the LIBESS undergoes several major discharge cycles to cooperatively keep with DGs the supply-demand balance in the MG. The LIB reaches the maximum discharged energy of 153.1 kWh, which is the required LIB capacity for energy management in the islanded operation. In

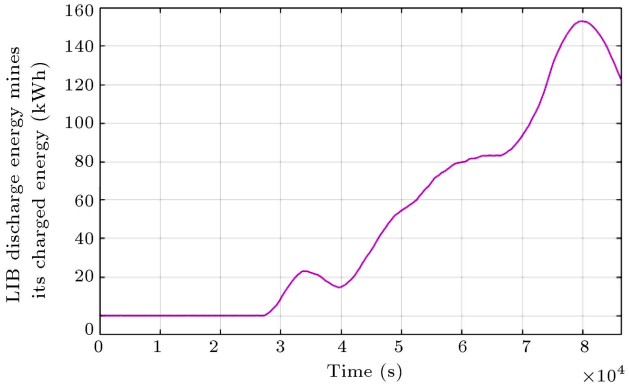

Figure 16. Discharged energy of LIB minus its charged energy.

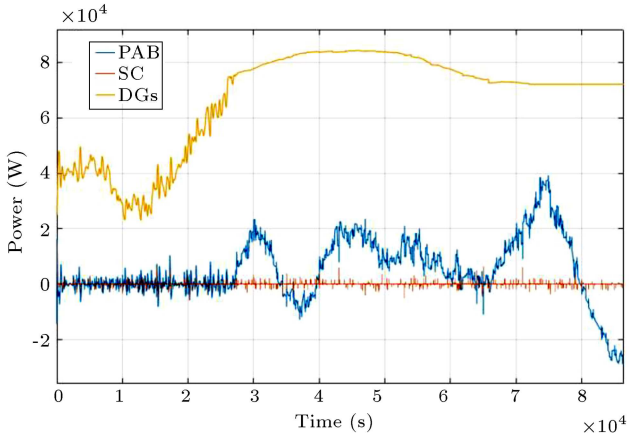

Figure 17. PSHESS and DGs power.

addition, the LIB power reaches the maximum value of 38.65 kW. From $t = 34399$ sec until $t = 39567$ sec, the LIB goes through a charge cycle to absorb the extra-generated energy by DGs so that its SOC is restored at SOC_{LIB}^{ref} and the required LIB capacity is minimized.

3.3.2. Energy management with PSHESS

Figure 17 shows the power of the SC, LIB, and DGs. Energy management with PSHESS almost resembles that with LIBESS, except that the SC and PAB of the PSHESS deal with FCMFVs and SCMFVs, respectively, while the LIBESS deals with both of them in the previous section. Figure 18 shows the discharged energy of the PAB minus its charged energy, which is quite similar to that of LIB in Figure 16, indicating negligible discharged/charged energy of SC. From $t = 27200$ sec to $t = 79761$ sec, the PAB undergoes several major discharge periods. The LIB has reached the maximum discharged energy of 153.098 kWh, which is the required LIB capacity for energy management in the islanded operation. The negligible difference between the maximum discharged energy of the PAB (153.098 kWh) and that of the LIB (153.1 kWH), which is 0.002 kWh, results from the performance of the SC that deals with FCMFVs. The PAB power reached the maximum value of 37.43 kW. The maximum discharged

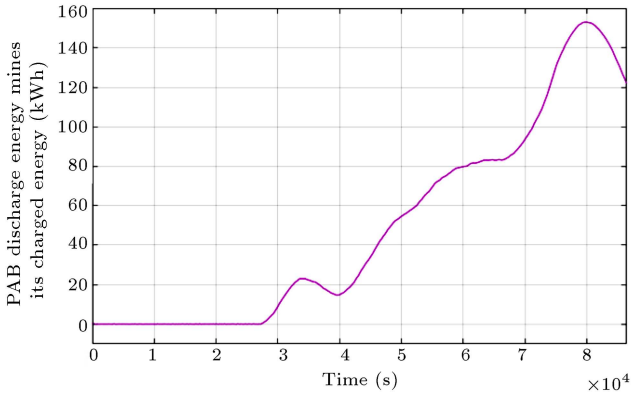

Figure 18. Discharged energy of the PAB minus its charged energy.

power of the PSHESS is 38.65 kW. The needed capacity of the PAB is 61.19 kWh, which is the maximum injected energy of the LIB during the whole simulation time. Of note, the maximum continuous charged and discharged energies of the SC are 0.53 Wh and 0.46 Wh, respectively.

3.4. Cost comparison between LIBESS and PSHESS

Eq. (2) calculates the cost of PSHESS (C_{PSHESS}), which includes the costs of the PAB, SC, and an inverter and two converters:

$$C_{PSHESS} = (BC_{SC}.RC_{SC}) + (BC_{PAB}.RC_{PAB}) + (BC_{Con}.RP_{PABCon}) + (BC_{Con}.RP_{SCCon})(BC_{Inv}.RP_{Inv}) \quad (3.1)$$

where BC_{SC} and RC_{SC} are the base cost (\$/kW.h) and nominal capacity (kW.h) of the SC, respectively; BC_{PAB} and RC_{PAB} are the base cost (\$/kW.h) and nominal capacity (kW.h) of the PAB, respectively; BC_{Con} is the converter base cost (\$/kW); RP_{SCCon} and RP_{PABCon} represent the nominal powers (kW) of the converters connected to the SC and the PAB, respectively; and BC_{Inv} and RP_{Inv} stand for the base cost (\$/kW) and inverter nominal power (kW), respectively. The nominal capacity of the PAB (RC_{PAB}) can be obtained using Eq. (3):

$$RC_{PAB} = \frac{E_{\max Dis}^{PAB}}{\eta_{Conv}.\eta_{Inv}}, \quad (3.2)$$

where η_{Conv} and η_{Inv} are the converter and inverter efficiencies, respectively, and the values of both are equal to 0.9 [44,45]. In addition, $E_{\max Dis}^{PAB}$ is the maximum injected energy of the PAB during energy management simulation studies, which is 61.19 kWh.

The cost of an PAB cell that can perform 2000 life cycles is 600 \$/kWh [46]. As stated in [47], the hybrid application of both PABs and SC results in 30% PABs

life extension. In other words, the PAB can perform 30% more life cycles in the case of being hybridized with the SC. Assuming that the PAB performs one full discharge/charge cycle every day, as proposed in [48], we can calculate BC_{PAB} for a decade of operation using Eq. (4):

$$BC_{LAB} = \frac{600\$}{2000 life\_cycles \times 1.3} \times 3650 cycles \cong 842.31\ \$/\text{lWh}. \quad (3.3)$$

The SC should have enough charged/uncharged capacity to inject/absorb the maximum needed energy to intercept frequency deviation in the worst cases of power shortage/surplus. The needed charged capacity of the SC ($E^{SC}_{\max Dis}$) is equal to the maximum injected energy of the SC during the frequency regulation studies, which is 5.6648 Wh. It is assumed that the severity of the power surplus scenario that the MG ever experiences is the same as that of the worst power shortage scenario. Therefore, the needed uncharged capacity ($E^{SC}_{\max Cha}$) is also considered to be equal to $E^{SC}_{\max Dis}$. Eq. (5) presents the formulation for calculating the needed SC capacity:

$$E_{SC} = \frac{(E^{SC}_{\max Dis} + E^{SC}_{\max Cha})}{\eta_{Conv}.\eta_{Inv}} = \frac{2.E^{SC}_{\max Dis}}{\eta_{Conv}.\eta_{Inv}}. \quad (3.4)$$

For a decade of operation, the value of BC_{SC} is 15000 \$/kW [49]. The power ratings of the converters of the PAB and SC are equal to the maximum powers passing through them, which are 37.43 kW and 27.61 kW, respectively. Considering the inverter efficiency, which is not considered in the simulation results, the inverter power rating can be obtained using Eqs. (6) and (7):

$$RP_{SCCon} = \frac{P^{\max}_{SC}}{\eta_{Inv}}, \quad (3.5)$$

$$RP_{PABCon} = \frac{P^{\max}_{LAB}}{\eta_{Inv}}, \quad (3.6)$$

where $P^{\max}_{SC}$ and $P^{\max}_{PAB}$ are the maximum injected/absorbed power of the SC and PAB, respectively, and BC_{Con} is 50 \$/kW [49]. The PSHESS inverter power rating is 38.65 kW which is the maximum power passing through it during the FCEM studies. Of note, the value of BC_{Inv} is 600 \$/kWh [50].

Eq. (8) calculates the cost of LIBESS, which consists of the costs of the LIB, inverter, and two converters:

$$C_{LIBESS} = (BC_{LIB}.RC_{LIB}) + (BC_{Con}.RP_{LIBCon}) + (BC_{Inv}.RP_{Inv}), \quad (3.7)$$

where RC_{LIB} and BC_{LIB} are the base cost (\$/kWh) and the nominal capacity (kWh) of the LIB, respectively, and RP_{LIBCon} and RP_{Inv} are the nominal power of the converter and inverter of the LIB, respectively. From the energy management simulation studies, the maximum injected energy of the LIB ($E^{LIB}_{\max Dis}$) is 153.1 kWh. Here, RC_{LIB} can be obtained through Eq. (9):

$$RC_{LIB} = \frac{E^{LIB}_{\max Dis}}{\eta_{Inv}.\eta_{Conv}}. \quad (3.8)$$

The LIB cost with 6000 life cycles is 1000 \$/kwh [46]. Assuming that the LIB performs one full discharge/charge cycle each day, as proposed in [48], the value of BC_{LIB} can be calculated for a decade of operation using Eq. (10):

$$BC_{LIB} = \frac{1000\$}{6000 life\_cycles} \times 3650 cycles \cong 608.34\ \$/\text{kWh}. \quad (3.9)$$

The maximum injected/absorbed power of LIB ($P^{\max}_{LAB}$) in the FCEM studies is 38.65 kW. Therefore, RP_{LIBCon} can be calculated using Eq. (11):

$$RP_{LIBCon} = \frac{P^{\max}_{LAB}}{\eta_{Inv}}. \quad (3.10)$$

RP_{Inv} is 38.65 kW which is the maximum power passing through it during the FCEM studies.

Based on Eqs. (2)–(11) and the numerical results from the simulations, Table 1 lists the sizes of the components of the LIBESS, PSHESS, and their base costs.

Based on the data available in Table 1 and

Table 1. Summarized data of sizing and cost calculation of LIBESS and PSHESS.

LIBESS		PSHESS	
Item	**Value**	**Item**	**Value**
RC_{LIB} (kWh)	189.02	RC_{PAB} (kWh)	189.01
BC_{LIB} (\$/kWh)	608.34	BC_{PAB} (\$/kWh)	842.31
RP_{LIBCon} (kW)	42.95	E_{SC} (Wh)	13.99
BC_{Con} (\$/kW)	50	BC_{SC} (\$/kWh)	15000
RP_{Inv} (kW)	38.65	RP_{SCCon} (kW)	30.68
BC_{Inv} (\$/kW)	600	RP_{PABCon} (kW)	41.59
		RP_{Inv} (kW)	38.65

Eqs. (2) and (8), the total costs of the LIBESS and PSHESS are calculated as \$140325.93 and \$209408.37, respectively. The cost evaluation of the LIBESS and PSHESS indicates that for a decade of operation, the cost of the PSHESS is almost 49.2% more than that of the LIBESS, mainly because the LIB cost per each life cycle is more than that of the PAB, thus decreasing the LIBESS cost. Compared to the PSHESS configuration, the LIBESS requires one less converter and also, it does not require an SC. Unlike the PSHESS, the control system of the LIBESS does not require high-pass and low-pass filters to separate SCMFVs from FCMFVs. Therefore, the LIBESS is technically and economically more suitable than the PSHESS in the case of the islanded operation of the MG.

4. Conclusion

The current research initially remarked that the LIBESS with high power and high energy densities could function like a Pb-acid battery-Supercapacitor Hybrid ESS (PSHESS). Given that the LIBESS and PSHESS are two common ESS technologies, a techno-economic comparison was made to determine the superior candidate for the islanded operation of an Micro-Grid (MG). In this regard, two Frequency Control and Energy Management (FCEM) schemes were proposed using the LIBESS and PSHESS. Regarding the PSHESS, high-pass and low-pass filters were used to separate the FCMFVs and SCMFVs in the frequency controllers of the Super capacitor (SC) and Pb-Acid Battery (PAB). In doing so, the stress of the fast power regulations on the PAB of the PSHESS as the SC handled fast power regulations would decrease, while the PAB dealt with slow power regulation. The frequency controllers of the LIBESS and SC of the PSHESS were tuned to ensure the constant MG frequency maintenance within the allowable range. The proposed FCEM used the coordinated application of the ESSs and Distributed Generators (DGs) to maintain the supply-demand balance, which led to the least utilization and needed sizes of the Lithium-Ion Battery (LIB) and PAB for the energy management of the MG during the islanded operation. Based on the proposed FCEM schemes as well as energy management and frequency regulation studies, the sizes and costs of the LIBESS and PSHESS were determined to be \$140325.93 and \$209408.37, respectively. It was shown that the cost of the PSHESS was \$69082.44 which was almost 49.2% more than that of the LIBESS for a decade of operation, mainly due to the SC cost, low life-cost ratio of the PAB (compared to that of the LIB), and an extra needed converter (compared to the LIBESS topology). In addition, in comparison to the LIBESS, the topology and control system of the PSHESS were more complicated than those of the LIBESS. Therefore, the LIBESS was more efficient as an overriding choice than the PSHESS for the FCEM study of the islanded MG from the technical and economic points of view.

This paper economically analyzed the LIB and the PAB, considering that they are currently among the most widely used energy storage technologies. However, there are other sources including the superconducting magnetic energy storage. Therefore, it would be a good subject of study to analyze other storage technologies so that one of them might be economically more feasible than the two storage technologies investigated in this paper. The main focus of this study was put on the islanded operation of the MG while the storage technologies could also be applicable to the grid-connected operation, as well. Considering that the grid-connected operation is entirely different from the islanded operation, we recommend conducting a techno-economic study of the LIBESS and PSHESS for the grid-connected operation even though it is expected that the LIBESS will be more suitable than the PSHESS for this case too since the base cost of LIB is considerably less than that of PAB.

Nomenclature

BC_{Con}	Base cost of converter
BC_{LIB}	Base cost of LIB
BC_{SC}	Base cost of LIB of SC
C_{LIBESS}	Cost of LIBESS
DG	Distributed Generator
ESS	Energy Storage System
$E^{SC}_{\max Cha}$	Maximum charged energy of LIB
FCEM	Frequency Control and Energy Management
LIBESS	LIB ESS
MT	Microturbine
$P^{\max}_{PAB}$	Maximum power of PAB
$P^{\max}_{SC}$	Maximum injected/absorbed power of the SC
PV	Photovoltaic
RC_{LIB}	Rated capacity of LIB
RP_{Inv}	Rated power of inverter
RP_{PABCon}	Rated power of PAB converter
RP_{SCCon}	Rated power of SC converter
SOC_{LIB}	SOC of LIB
SOC_{PAB}	SOC of PAB
SOC_{SC}	SOC of SC
SOFC	Solid-oxide fuel cell
SCMFV	Slow Components of MG Frequency Variations
V_{DC}	Voltage of DC link

η_{Inv}	Inverter efficiency
BC_{Inv}	Base cost of converter
BC_{PAB}	Base cost of PAB
BESS	Battery ESS
C_{PSHESS}	Cost of PSHESS
DEG	Diesel Engine Generator
$E^{LIB}_{\max Dis}$	Maximum discharged energy of LIB
$E^{SC}_{\max Dis}$	Maximum discharged energy of SC
FCMFV	Fast Components of MG Frequency Variations
LIB	Lithium-Ion Battery
MG	Microgrid
PAB	Pb-Acid Battery
$P^{\max}_{PAB}$	maximum injected/absorbed power of the PAB
PSHESS	PAB-SC HESS
RC_{LIBCon}	Rated power of LIB converter
RC_{PAB}	Rated capacity of PAB
RC_{SC}	Rated capacity of SC
SC	Supercapacitor
SOC	State of Charge
SOC^{ref}_{LIB}	Reference value for SOC_{LIB}
SOC^{ref}_{PAB}	Reference value for SOC_{PAB}
SOC^{ref}_{SC}	Reference value for SOC_{SC}
V_{DCref}	Reference value for V_{DC}
η_{Conv}	Converter efficiency

References

1. Bagheri Sanjareh, M., Nazari, M.H., and Hosseinian, S.H. "A novel strategy for frequency control of islanded greenhouse with cooperative usage of BESS and LED lighting loads", *Electr. Eng.*, **103**(1), pp. 265–277 (2020).
2. Hirsch, A., Parag, Y., and Guerrero, J. "Microgrids: A review of technologies, key drivers, and outstanding issues", *Renew. Sustain. Energy Rev.*, **90**, pp. 402–411 (2018).
3. Sanjareh, M.B., Nazari, M.H., Ghiasi, N., et al. "New strategy for battery sizing regarding the impact of discharge durations on its capacity", *2021 29th Iran. Conf. Electr. Eng.*, pp. 329–334 (2021).
4. Sanjareh, M.B., Nazari, M.H., Gharehpetian, G.B., et al. "A novel strategy for optimal battery sizing based on MG frequency security criterion", *2019 Int. Power Syst. Conf.*, pp. 716–722 (2019).
5. Ke, B.R., Lin, Y.H., Chen, H.Z., et al. "Battery charging and discharging scheduling with demand response for an electric bus public transportation system", *Sustain. Energy Technol. Assessments*, **40**, 100741 (2020).
6. Singh, P. and Lather, J.S. "Power management and control of a grid-independent DC microgrid with hybrid energy storage system", *Sustain. Energy Technol. Assessments*, **43**, 100924 (2021).
7. Bagheri-Sanjareh, M., Nazari, M.H., and Hosseinian, S.H. "Coordination of hybrid energy storage system, photovoltaic systems, smart lighting loads, and thermostatically controlled loads for microgrid frequency control", *Int. Trans. Electr. Energy Syst.*, **31**(8), pp. 1–27 (2021).
8. El-houari, H., Allouhi, A., Salameh, T., et al. "Energy, Economic, Environment (3E) analysis of WT-PV-Battery autonomous hybrid power plants in climatically varying regions", *Sustain. Energy Technol. Assessments*, **43**, 100961 (2021).
9. Hajiaghasi, S., Salemnia, A., and Hamzeh, M. "Hybrid energy storage system for microgrids applications: A review", *J. Energy Storage*, **21**, pp. 543–570 (2019).
10. Branco, H., Castro, R., and Setas Lopes, A. "Battery energy storage systems as a way to integrate renewable energy in small isolated power systems", *Energy Sustain. Dev.*, **43**, pp. 90–99 (2018).
11. Dhundhara, S., Verma, Y.P., and Williams, A. "Techno-economic analysis of the lithium-ion and lead-acid battery in microgrid systems", *Energy Convers. Manag.*, **177**, pp. 122–142 (2018).
12. Deveau, J., White, C., and Swan, L.G. "Lead-acid battery response to various formation levels - Part A: Recommended formation levels for off-grid solar and conventional applications", *Sustain. Energy Technol. Assessments*, **11**, pp. 1–10 (2015).
13. May, G.J., Davidson, A., and Monahov, B. "Lead batteries for utility energy storage: A review", *J. Energy Storage*, **15**, pp. 145–157 (2018).
14. Jing, W., Lai, C.H., Wong, W.S.H., et al. "A comprehensive study of battery-supercapacitor hybrid energy storage system for standalone PV power system in rural electrification", *Appl. Energy*, **224**, pp. 340–356 (2018).
15. Cabrane, Z., Ouassaid, M., and Maaroufi, M. "Analysis and evaluation of battery-supercapacitor hybrid energy storage system for photovoltaic installation", *Int. J. Hydrogen Energy*, **41**(45), pp. 20897–20907 (2016).
16. Cohen, I.J., Wetz, D.A., Heinzel, J.M., et al. "Design and characterization of an actively controlled hybrid energy storage module for high-rate directed energy applications", *IEEE Trans. Plasma Sci.*, **43**(5), pp. 1427–1433 (2014).
17. Ahmadi, L., Fowler, M., Young, S.B., et al. "Energy efficiency of Li-ion battery packs re-used in stationary power applications", *Sustain. Energy Technol. Assessments*, **8**, pp. 9–17 (2014).
18. Abdin, Z. and Khalilpour, K.R. "Single and polystorage technologies for renewable-based hybrid energy systems", In *Polygeneration with Polystorage for Chemical and Energy Hubs*, Elsevier, pp. 77–131 (2019).

19. Sanjareh, M.B., Nazari, M.H., Gharehpetian, G.B., et al. "A novel approach for sizing thermal and electrical energy storage systems for energy management of islanded residential Microgrid", *Energy Build.*, **238**, p. 110850 (2021).
20. Bagheri-Sanjareh, M. and Nazari, M.H. "Coordination of energy storage system, PVs and smart lighting loads to reduce required battery size for improving frequency response of islanded microgrid", *Sustain. Energy, Grids Networks*, **22**, 100357 (2020).
21. Jenu, S., Deviatkin, I., Hentunen, A., et al. "Reducing the climate change impacts of lithium-ion batteries by their cautious management through integration of stress factors and life cycle assessment", *J. Energy Storage*, **27**, 101023 (2020).
22. Omar, N., Monem, M.A., Firouz, Y., et al. "Lithium iron phosphate based battery-assessment of the aging parameters and development of cycle life model", *Appl. Energy,* **113**, pp. 1575–1585 (2014).
23. Ceraolo, M., Lutzemberger, G., and Poli, D. "Aging evaluation of high power lithium cells subjected to micro-cycles", *J. Energy Storage*, **6**, pp. 116–124 (2016).
24. Wen, S., Wang, S., Liu, G., et al. "Energy management and coordinated control strategy of PV/HESS AC microgrid during Islanded operation", *IEEE Access*, **7**, pp. 4432–4441 (2018).
25. Kerdphol, T., Qudaih, Y., and Mitani, Y. "Optimum battery energy storage system using PSO considering dynamic demand response for microgrids", *Int. J. Electr. Power Energy Syst.*, **83**, pp. 58–66 (2016).
26. Kerdphol, T., Fuji, K., Mitani, Y., et al. "Optimization of a battery energy storage system using particle swarm optimization for stand-alone microgrids", *Int. J. Electr. Power Energy Syst.*, **81**, pp. 32–39 (2016).
27. Bagheri-Sanjareh, M., Nazari, M.H., and Gharehpetian, G.B. "A novel and optimal battery sizing procedure based on MG frequency security criterion using coordinated application of BESS, LED lighting loads, and photovoltaic systems", *IEEE Access*, **8**, pp. 95345–95359 (2020).
28. Mateska, A.K., Borozan, V., Krstevski, P., et al. "Controllable load operation in microgrids using control scheme based on gossip algorithm", *Appl. Energy*, **210**, pp. 1336–1346 (2018).
29. Das, B. and Kumar, A. "Cost optimization of a hybrid energy storage system using GAMS", *2017 Int. Conf. Power Embed. Drive Control, IEEE*, pp. 89–92 (2017).
30. Gbadegesin, A.O., Sun, Y., and Nwulu, N.I. "Techno-economic analysis of storage degradation effect on levelised cost of hybrid energy storage systems", *Sustain. Energy Technol. Assessments*, **36**, 100536 (2019).
31. Rizvandi, A.K., Bagheri Sanjareh, M., Nazari, M.H., et al. "A novel scheme for enabling air conditioners to participate in primary frequency control-IEEE conference publication", *10th Smart Grid Conf.*, IEEE, Tehran (2020).
32. Bagheri-Sanjareh, M., Nazari, M.H., and Hosseinian, S.H. "Energy management of islanded microgrid by coordinated application of thermal and electrical energy storage systems", *Int. J. Energy Res.*, **45**(4) (n.d.).
33. Patel, J., Chandwani, H., Patel, V., et al. "Bi-directional DC-DC converter for battery charging-Discharging applications using buck-boost switch", In *2012 IEEE Students' Conference on Electrical, Electronics and Computer Science*, pp. 1–4 IEEE, https://doi. org/10.1109/SCEECS (2012).
34. Bahrani, B., Kenzelmann, S., and Rufer, A. "Multivariable-PI-based *dq* current control of voltage source converters with superior axis decoupling capability", *IEEE Trans. Ind. Electron.*, **58**(7), pp. 3016–3026 (2010).
35. Sanjareh, M.B., Nazari, M.H., Gharehpetian, G.B., et al. "Optimal scheduling of HVACs in islanded residential microgrids to reduce BESS size considering effect of discharge duration on voltage and capacity of battery cells", *Sustain. Energy, Grids Networks*, **25**, 100424 (2020).
36. Jumani, T.A., Mustafa, M.W., Md Rasid, M., et al. "Optimal voltage and frequency control of an islanded microgrid using grasshopper optimization algorithm", *Energies*, **11**(11), p. 3191 (2018).
37. Wu, D., Tang, F., Dragicevic, T., et al. "Autonomous active power control for islanded AC microgrids with photovoltaic generation and energy storage system", *IEEE Trans. Energy Convers.*, **29**(4), pp. 882–892 (2014).
38. Karimi-Rizvandi, A., Sandjareh, M.B., Nazari, M.H., et al. "A novel frequency control scheme for autonomous microgrid using cooperative application of supercapacitor-battery HESS, photovoltaics, LED lighting loads and TCLs", *IEEE Access*, **9**, pp. 57198–57214 (2021).
39. Friedel, V., *Modeling and Simulation of a Hybrid Wind-Diesel Microgrid* (2009).
40. Zhu, Y. and Tomsovic, K. "Development of models for analyzing the load-following performance of microturbines and fuel cells", *Electr. Power Syst. Res.*, **62**(1), pp. 1–11 (2002).
41. Kim, Y.-S., Kim, E.-S., and Moon, S.-I. "Frequency and voltage control strategy of standalone microgrids with high penetration of intermittent renewable generation systems", *IEEE Trans. Power Syst.*, **31**(1), pp. 718–728 (2015).
42. Nazari, M.H., Bagheri Sanjareh, M., Mohammadian, M., et al. "A novel economic model for enhancing technical conditions of microgrids and distribution networks utilizing an iterative cooperative game-based algorithm", *Sustain. Energy Technol. Assessments*, **45**, 101135 (2021).
43. Kermanshahi, B. and Kamel, R.M. "Design and Implementation of Models for Analyzing the Dynamic Performance of Distributed Generators in the

Micro Grid Part I: Micro Turbine and Solid Oxide Fuel Cell", *Scientia Iranica*, **17**(1), pp. 47–58 http://scientiairanica.sharif.edu/article_3310.html.

44. Wang, C., Xiong, R., He, H., et al. "Efficiency analysis of a bidirectional DC/DC converter in a hybrid energy storage system for plug-in hybrid electric vehicles", *Appl. Energy*, **183**, pp. 612–622 (2016).

45. Bordin, C., Anuta, H.O., Crossland, A., et al. "A linear programming approach for battery degradation analysis and optimization in offgrid power systems with solar energy integration", *Renew. Energy*, **101**, pp. 417–430 (2017).

46. Xie, Z., Du, L., Lv, X., et al. "Evaluation and analysis of battery technologies applied to grid-level energy storage systems based on rough set theory", *Trans. Tianjin Univ.*, **26**, pp. 1–8 (2020).

47. Carter, R., Cruden, A., and Hall, P.J. "Optimizing for efficiency or battery life in a battery/supercapacitor electric vehicle", *IEEE Trans. Veh. Technol.*, **61**(4), pp. 1526–1533 (2012).

48. Rydh, C.J. and Sandén, B.A. "Energy analysis of batteries in photovoltaic systems. Part I: Performance and energy requirements", *Energy Convers. Manag.*, **46**(11–12), pp. 1957–1979 (2005).

49. Masih-Tehrani, M., YAZDI, M.R.H., Esfahanian, V., et al. "Wavelet-based power management for hybrid energy storage system", *J. Mod. Power Syst. Clean Energy*, **7**(4), pp. 779–790 (2019).

50. Ghenai, C. and Bettayeb, M. "Design and optimization of grid-tied and off-grid solar PV systems for super-efficient electrical appliances", *Energy Efficiency*, **13**, pp. 1–15 (2019).

Biographies

Ahmad Karimi-Rizvandi was born in Iran. He has received his BSc and MSc degrees from Shahed university and Iran University of Science and Technology, Tehran, Iran, respectively. His research interests include planning, operation, energy management, and control of the micro grids as well as the grid integration of the distributed and renewable resources, and smart grids.

Mehrdad Bagheri-Sanjareh was born in Iran. He received the BSc degree from Shahed University, Tehran in 2014 and MSc degree from Shahid Beheshti University, Tehran in 2017. His research interests include smart grids, energy storage systems, distributed generators, energy markets, power system optimization, power quality, planning and power system stability, and control. He has published numerous conference and journal papers and has been involved in several research projects related to these fields.

Mohammad Hassan Nazari received his MSc degree in Power Electrical Engineering at Sharif University of Technology in 2013, and his PhD degree in power system engineering at the Tehran Amirkabir polytechnic, Tehran, Iran in 2020. He is currently working as Postdoctoral Researcher at the Electrical Engineering Department, Tehran Polytechnic. His research interests include power system optimization, renewable and fossil-fuel-based resource management, energy pricing, frequency control, and resilience improvement of microgrids.

Gevork B. Gharehpetian received his PhD degree in Electrical Engineering from Tehran University, Tehran in 1996. As a PhD student, he has received scholarship from DAAD (German Academic Exchange Service) from 1993 to 1996. He was with the High Voltage Institute, RWTH Aachen, Aachen, Germany. From 1997 to 2003, he was an Assistant Professor at AUT, Associate Professor from 2004 to 2007, and Professor since 2007. Based on the Web of Science database (2005–2019), he is among world's top 1% elite scientists according to the Essential Science Indicators (ESI) ranking system. He is the author of more than 1200 journal articles and conference papers.

Seyed Hossein Hosseinian received the PhD degree from the University of Newcastle, Newcastle, England in 1995. He is currently a Full Professor with the Electrical Engineering Department, Tehran Polytechnic, Tehran, Iran. Based on the Web of Science database, he is among world's top 1% elite scientists according to Essential Science Indicators (ESI) ranking system.